HHS Public Access

Author manuscript

Neuroimage. Author manuscript; available in PMC 2022 February 20.

Published in final edited form as:

Neuroimage. 2020 December ; 223: 117343. doi:10.1016/j.neuroimage.2020.117343.

Manganese-enhanced MRI reveals changes within brain anxiety and aversion circuitry in rats with chronic neuropathic pain- and anxiety-like behaviors

Sabrina L. McIlwrath[a,*], **Marena A. Montera**[b,1], **Katherine M. Gott**[b,1], **Yirong Yang**[b,2], **Colin M. Wilson**[b,3], **Reed Selwyn**[b,3], **Karin N. Westlund**[a,b,1]

[a]Research Services New Mexico VA HealthCare System Albuquerque NM 87108 USA

[b]University of New Mexico Health Sciences Center, Albuquerque, NM USA

Abstract

Chronic pain often predicts the onset of psychological distress. Symptoms including anxiety and depression after pain chronification reportedly are caused by brain remodeling/recruitment of the limbic and reward/aversion circuitries. Pain is the primary precipitating factor that has caused opioid overprescribing and continued overuse of opioids leading to the current opioid epidemic. Yet experimental pain therapies often fail in clinical trials. Better understanding of underlying pathologies contributing to pain chronification is needed to address these chronic pain related issues. In the present study, a chronic neuropathic pain model persisting 10 weeks was studied. The model develops both anxiety- and pain-related behavioral measures to mimic clinical pain. The manganese-enhanced magnetic resonance imaging (MEMRI) utilized improved MRI signal contrast in brain regions with higher neuronal activity in the rodent chronic constriction trigeminal nerve injury (CCI-ION) model. T1-weighted MEMRI signal intensity was increased compared to controls in supraspinal regions of the anxiety and aversion circuitry, including anterior cingulate gyrus (ACC), amygdala, habenula, caudate, ventrolateral and dorsomedial periaqueductal gray (PAG). Despite continuing mechanical hypersensitivity, MEMRI T1 signal intensity as the neuronal activity measure, was not significantly different in thalamus and decreased in somatosensory cortex (S1BF) of CCI-ION rats compared to naïve controls. This is consistent with decreased fMRI BOLD signal intensity in thalamus and cortex of patients with longstanding trigeminal neuropathic pain reportedly associated with gray matter volume decrease in these regions. Significant increase in MEMRI T2 signal intensity in thalamus of CCI-ION

[*]Corresponding author. sabrina.mcilwrath@va.gov (S.L. McIlwrath).
[1]Anesthesiology
[2]College of Pharmaceutical Sciences
[3]Department of Radiology

Author contributions

S.L.M. performed the animal experiments, data analysis, produced the figures, wrote the manuscript. M.A.M. assisted in animal $MnCl_2$ dosing and performed MEMRI data analysis. K.M.G. wrote the UNM IACUC protocol, coordinated animal transfer between facilities and scheduled MEMRIs. C.M.W. and R.S. assisted in MEMRI data analysis. K.N.W. designed the study, read and edited this manuscript. All authors discussed the results, read and edited the manuscript.

Declaration of Competing Interest

No authors have conflicts of interest.

Supplementary materials

Supplementary material associated with this article can be found, in the online version, at doi:10.1016/j.neuroimage.2020.117343.

animals was indication of tissue water content, cell dysfunction and/or reactive astrogliosis. Decreased T2 signal intensity in S1BF cortex of rats with CCI-ION was similar to findings of reduced T2 signals in clinical patients with chronic orofacial pain indicating prolonged astrocyte activation. These findings support use of MEMRI and chronic rodent models for preclinical studies and therapeutic trials to reveal brain sites activated only after neuropathic pain has persisted in timeframes relevant to clinical pain and to observe treatment effects not possible in short-term models which do not have evidence of anxiety-like behaviors. Potential improvement is predicted in the success rate of preclinical drug trials in future studies with this model.

Keywords

Magnetic resonance imaging; Neuropathic pain; Chronic pain; Trigeminal nerve; Orofacial pain; CCI-ION; Depression; Pain matrix

1. Introduction

Chronic head and/or neck pains account for over 23% of complaints among Americans, and of these less than 30% can be effectively treated by current therapies (Nahin, 2017). Trauma to the head damaging the trigeminal nerve caused by blunt force, sports and vehicular accidents, or exposure to explosions, can lead to chronic orofacial neuropathic pain. Decades of study indicate that complex, multifactorial mechanisms are responsible for generating and maintaining neuropathic pain, a process referred to as the “chronification” of pain (Ossipov et al., 2014; McCarberg and Peppin, 2019). This process is thought to involve molecular, physiological, neuroplastic, and even anatomical alterations, resulting in brain remodeling that includes recruitment of limbic and aversion circuitries (Lu et al., 2016; Danaher et al., 2018; Lapaglia et al., 2018; Ong et al., 2019). Functional magnetic resonance imaging (fMRI) scans of patients with chronic back pain identified altered brain circuitry in amygdala, medial prefrontal cortex/anterior cingulate gyrus (mPFC/ACC), and hippocampus within 3–12 months that correlated with pain level and duration (Baliki et al., 2012; Hashmi et al., 2013). Chronic pain can cause functional reorganization of the brain as well as reduction of gray matter volume in distinct cortical regions due to central plasticity that can recover once pain is alleviated (May, 2008; Mansour et al., 2013; Mutso et al., 2014). Chronic pain causing concurrent activation of emotional brain circuits can produce secondary dysfunctional affective/emotional symptoms such as anxiety, depression, and altered cognitive function (Seminowicz et al., 2009; Hashmi et al., 2013; Borsook et al., 2016). Similarly, following the trigeminal infraorbital nerve chronic constriction injury model (CCI-ION) in rats through ten weeks has provided the data presented here for both mechanical hypersensitivity and anxiety-related behaviors. Further, the model has provided manganese enhanced magnetic resonance imaging (MEMRI) data indicating brain activation in emotional brain circuitry.

MEMRI has been widely used for high contrast imaging in anesthetized rodents since the 1990s. Due to the biochemical similarity of Mn^{2+} and Ca^{2+} ions, Mn^{2+} can enter neurons and other excitable cells through several types of Ca^{2+} channels, including voltage-gated Ca^{2+} channels and the Na^{+}/Ca^{2+} exchanger (Lin and Koretsky, 1997; Takeda, 2003; Bedenk

et al., 2018). Manganese ions are paramagnetic and, upon uptake, shorten tissue longitudinal or spin-lattice relaxation times (T1), and improve MRI signal contrast thus enhancing brain cytoarchitecture for anatomical studies (Masaad and Paulter, 2011). Increased MEMRI T1 signal is indicative of brain regions with higher neuronal activity (Alshelh et al., 2018). This activity dependent uptake of Mn^{2+} and resulting MEMRI tissue contrast are more directly related to neural activity than fMRI BOLD signal (Paulter, 2004; Soria et al., 2008). MEMRI has been used in several animal models of acute, persistent, and chronic somatic pain. Increased T1 signals have been identified after acute noxious stimulation in primary sensory and insular cortices (Cha et al., 2016). After chronic neuropathic pain, T1 signal has identified volume shrinkage in several cortical areas including primary sensory, anterior cingulate, and insular cortices (Seminowicz et al., 2009). In contrast, increased transverse or spin-spin relaxation times (T2 signal) can indicate higher water content due to edema and decreases can be caused by Mn^{2+} uptake and/or reactive astrogliosis (Kawai et al., 2010; Malheiros et al., 2014; Alshelh et al., 2018). Analyses of both T1 and T2 signal intensity in the present study provided data relevant to these prior findings.

The current study in anesthetized male rats with chronic neuropathic orofacial pain induced by the CCI-ION model with concurrent anxiety-related behavioral changes, investigated brain activity increases in limbic and aversion related brain regions measurable by MEMRI with comparisons to matched naïve controls.

2. Materials and methods

2.1. Animals

All animal experiments were approved by the New Mexico Veteran's Administration Health Care System Animal Component of Research Protocol (ACORP 16-A214) and performed in accordance with the National Institute of Health Guide for the Care and Use of Laboratory Animals (NIH Publications No. 80–23) revised 1996. MEMRI imaging procedures were additionally approved by the Institutional Animal Care and Use Committee of the University of New Mexico (IACUC #17–200,613-HSC). Adult male Sprague-Dawley rats (125–150 g, Envigo, Indianapolis, IN, USA) were housed on 12/12 h reverse light cycle and fed ad libitum with a soy protein-free diet (Teklad #2920x, Envigo). All experimental procedures took place during the dark cycle after animals were acclimated for 2 weeks to the changed diurnal rhythm and prior to baseline testing.

2.2. Surgery

A modification of the chronic CCI-ION model first developed by Vos et al. (1994) was used. Briefly, rats were anesthetized using isoflurane (induction at 5.0 vol%, maintenance at 2.0 - 4.0 vol% in oxygen, 1.0 L/min; (Clipper Distributing, St. Joseph, MO, USA), the head above the left eye was shaved and then cleaned with povidone-iodine and 70% ethanol. Using aseptic procedures, the left ION was dissected free unilaterally within the orbital cavity. Two chromic gut sutures (5–0, Ethicon 634 G, Ethicon, Somerville, NJ, USA) were loosely tied around the left ION (2 mm apart) in the injured group ($N = 6$). In sham operated animals ($N = 6$) the ION was exposed but not ligated, while the naïve group ($N = 6$) did not undergo surgery nor anesthesia (Ma et al., 2012). The incision was closed using 5–0 nylon suture

(Cat. # MV-661, Med-Vet International, Mettawa, IL, USA). Animals were fully recovered from anesthesia within 15 min following surgery. Wound condition, body weights, and general activity were closely monitored post-surgery. No excessive body weight loss (>20% weight loss) was noted post-surgery and all animals thrived during the 11-week study.

3. Behavioral tests

All behavioral tests occurred after a 30 min acclimatization period in the testing room.

3.1. Assessment of mechanical hypersensitivity using reflexive tests

Weekly bilateral whisker pad measurements of the mechanical withdrawal thresholds were performed throughout the 11-week time course by a person blinded to experimental groups as described previously (Kaushal et al., 2016). Animals were acclimated to being held, gently wrapped in a towel, for 10 min prior to testing to minimize stress-induced effects (Aloisi et al., 1994). A series of 8 von Frey filaments exerting 0.4, 0.6, 1.0, 2.0, 4.0, 6.0, 8.0, 15.0 g force (Stoelting, Wood Dale, IL, USA) was used to determine the mechanical sensitivity of the vibrissal whisker pad using the up-down method (Ma et al., 2012). Testing always started with the 4.0 g force exerting filament. Each filament was applied 5 times perpendicular to the whisker pad at several second intervals while avoiding direct vibrissal stimulation. If a positive response (head withdrawal in 3 of 5 stimulations) was observed, then the next weaker filament was applied. In case of a negative response the next stronger von Frey filament was applied. After a positive response, testing continued in this manner until a further 4 fibers were applied, allowing the calculation of the mechanical withdrawal threshold using a curve fitting algorithm (Chaplan et al., 1994). A withdrawal threshold decrease indicated mechanical allodynia.

3.2. Assessment of anxiety-like behaviors with the light-dark place preference test

Rats were placed into a two-chambered plastic box (total size 27 x 27 cm) with free access between chambers through an open portal (6.5 x 6.5 cm) as previously described (Kline et al., 2015). One chamber was completely dark and the other brightly illuminated with a fluorescent bulb lamp (700 lumen). Animals were initially placed in the bright chamber and their behaviors recorded for 600 s (10 min) without investigators present. Post hoc analysis of video recorded behaviors quantified the number of entries into the light chamber. Entries were defined as the animal placing all 4 paws into the light chamber. Other measures analyzed included time spent in the illuminated chamber (*sec*), number of rearing events, and time spent rearing in the light chamber (*sec*).

3.3. Assessment of anxiety-like behaviors with the elevated plus maze

The elevated plus maze consists of two open and two closed arms elevated 60 cm from the floor. The open corridors are 110 cm long, the closed arms are each 50 cm long, and the widths are 10 cm. The closed arm's height is 40 cm. The rat is placed into the open 10 x 10 cm center square. Movements are video recorded for 5 min for off-line post hoc analysis, and then the rat is returned to its home cage. The numbers of center, open and closed arm entries; number of peeks into the open arms; total occupancy time in the center, open and closed arms; and number of exploratory rearing events in the closed arm are determined.

4. MEMRI

Only naïve and CCI-ION animal groups were scanned. Animals were injected intraperitoneally with 62 mg/kg manganese (II) chloride tetrahydrate (31 mg/ml $MnCl_2$ in 0.9% saline, pH 7.0, [Sigma-Aldrich, St. Louis, MO, USA]) 24 hrs prior to MRI scan to allow for even distribution throughout the brain (Aoki et al., 2004). Anesthesia was induced with 5% and maintained with 2–2.5% isoflurane (Clipper Distributing, St. Joseph, MO, USA) by mechanical ventilation. The animal was placed in a dedicated holder and positioned in the isocenter of a 7-Tesla MRI scanner equipped with a 30-cm bore, a 11.4 cm (inner diameter) 660 mT/m gradient, and an active shim system (Bruker Biospin, Billerica, MA, USA). A small bore quadrature radiofrequency (RF) coil (inner diameter = 86 mm) and a phased array surface coil were used for signal excitation and detection, respectively. Throughout the MRI scan time, respiration and heart rate were monitored, and body temperature was maintained at 37.0 ± 0.5 °C.

4.1. Fast low angle shot (FLASH)

The preclinical MRI software ParaVision 7 was used to determine T1 and T2 signal relaxation times in msec for the ROIs. The T1-weighted images were acquired using a fast sequence producing signals called gradient echo with low flip angles sequence (FLASH). The scan parameters were TR / TE = 500 ms / 3 ms, FOV = 3.5 cm x 3.5 cm, slice thickness = 0.5 mm, inter-slice distance = 0.5 mm, number of slices = 4, matrix = 256 × 256, number of average = 21. An in-house computer program in MATLAB (Mathworks), was used to determine signal intensities for the Region of Interest (ROI) listed below.

4.2. Rapid acquisition with relaxation enhancement (RARE)

The T2-weighted images were acquired using a fast spin-echo sequence with repetition time (TR) / echo time (TE) = 5, 500 ms / 33 ms, field of view (FOV) = 3.5 cm × 3.5 cm, slice thickness = 0.5 mm, inter-slice distance = 0.5 mm, number of slices = 4, matrix = 256 × 256, number of average = 3.

4.3. MEMRI data analysis

Brain ROIs were chosen a priori based on the literature on the pain neuraxis and brain regions activated by pain, anxiety and aversion in clinical patients and animal models (Ossipov et al., 2014; McCarberg and Peppin, 2019; Meda et al., 2019). They were identified according to Paxinos & Watson (1996). The ROIs included: left and right anterior cingulate cortex (ACC), amygdala (AMYG), caudate nucleus, dorsomedial periaqueductal gray (DMPAG), dentate gyrus (DEN), habenula (HAB), pyriform cortex (PYRC), primary sensory cortex barrel field (S1BF), thalamus (THAL), subthalamic regions medial dorsal nucleus (MD), thalamic reticular nucleus (TRN), and ventral posteromedial nucleus (VPM), ventrolateral periaqueductal gray (VLPAG), dorsal raphe nucleus (DRN), and ventral tegmental area (VTA). The MEMRI image data were exported to the VivoQuant 2.00 software (inviCRO, LLC, Boston, MA, USA) for image reconstruction, display, and analysis. Identical regional ROIs were used in all animals and T1 and T2 signal intensities collected. For each animal, data from each ROI were normalized to whole brain values

within each animal to eliminate coil artifacts and cohort differences (Chao et al., 2018). Data were then averaged for each experimental group.

5. Statistical analysis

Statistical analyses of the behavioral studies were performed with GraphPad Prism 6 software using one-way analyses of variance (ANOVA) with post hoc tests. Statistical analyses of MEMRI data were performed using MS Excel. Data outliers were identified by determining the median value for each ROI and then calculating the interquartile range. An outlier was defined as a data point 1.5 times above or below the third or first quartile. Two animals, a naïve control and a CCI animal, had more than 5 outlier data points and were removed from the analysis. The mean and SEM were then recalculated and Student's t-tests were used to determine significance. All brain regions were analyzed independently. Corrections for multiple t-tests were not performed to avoid a Type II error, loss of power to detect real differences (Saville, 1990). In all cases a $p \leq 0.05$ was considered significant.

6. Results

6.1. Mechanical threshold

The chromic gut suture used to induce the CCI-ION neuropathic pain model not only causes mechanical irritation of the peripheral nerve but also chemically induced inflammation (Maves et al., 1993). Animals with unilateral chronic constriction injury of the infraorbital nerve (CCI-ION) developed mechanical hypersensitivity on the ipsilateral whisker pad, the innervation territory. Within 3 weeks after the surgery, the decrease of the head withdrawal response thresholds to mechanical stimuli was maximal. Mechanical withdrawal thresholds on the ipsilateral side significantly decreased from 18.6 ± 0.1 g at baseline to 1.3 ± 0.2 g force in the CCI-ION group ($p < 0.05$, one-way ANOVA with Tukey's post hoc test, Fig. 1) while thresholds on the contralateral side did not change and remained between 18.5 ± 0.1 to 18.7 ± 0.0 g force. From week 3 until experiment end in week 10, head withdrawal thresholds on the ipsilateral side in CCI-ION animals were significantly lower (between 0.9 ± 0.1 and 1.3 ± 0.2 g force) compared to those of sham (between 16.3 ± 2.4 and 18.7 ± 0.0 g force) and naïve control animals (between 18.4 ± 0.2 and 18.7 ± 0.0 g force, $p < 0.05$, one-way ANOVA with Tukey's post hoc test, Fig. 1).

7. Anxiety-like behavior

In weeks 8 and 9, when hypersensitivity was chronic, anxiety-like behaviors were assessed using two different assays.

Light-dark place preference test.

In the light-dark place preference test, animals with CCI-ION injury entered the light side significantly less often (CCI-ION: 2.5 ± 1.1; naïve: 6.8 ± 1.7; sham: 6.5 ± 1.1; $p < 0.05$, one-way ANOVA on ranks) (Fig. 2A). Animals with CCI-ION spent significantly less time in the light chamber compared to naïve and sham control groups (CCI-ION: 39.8 ± 11.2 s; naïve: 112.0 ± 19.1 s; sham: 129.2 ± 19.8; $p < 0.001$, one-way ANOVA with Tukey's post hoc test) (Fig. 2B). The number of exploratory rearing events was significantly reduced in

the CCI-ION group (CCI-ION: 3.3 ± 1.4; naïve: 16.8 ± 2.2; sham: 14.7 ± 2.6; $p < 0.001$, one-way ANOVA with Tukey's post hoc test) (Fig. 2C). Also significantly reduced in the CCI-ION group was time spent rearing (CCI-ION: 17.5 ± 9.0 s; naïve: 41.2 ± 6.8 s; sham: 49.3 ± 8.4 s; $p < 0.05$, one-way ANOVA with Tukey's post hoc test) were (Fig. 2D).

Elevated plus maze.

In the elevated plus maze, animals with CCI-ION spent significantly less time in the maze center (CCI-ION: 2.0 ± 1.5; naïve: 5.8 ± 0.7; sham: 4.6 ± 2.5; $p < 0.05$, *t*-test) (Fig. 3A). They peeked less often into the open arm compared to naïve control animals, but not sham controls (CCI-ION: 14.6 ± 1.5; naïve: 31.0 ± 4.6; sham: 6.2 ± 3.6; $p < 0.05$, *t*-test) (Fig. 3B). Similarly, the number of entries into the closed arm of the CCI-ION group was significantly reduced compared to naïve controls, but not sham controls (CCI-ION: 1.6 ± 0.4; naïve: 6.2 ± 1.1; sham: 1.8 ± 0.5; $p < 0.05$, *t*-test) (Fig. 3C). No difference was determined for the number of rearing events (Fig. 3D) which all happened in the closed arm irrespective of experimental group (CCI-ION: 7.8 ± 0.5; naïve: 12.8 ± 1.3; sham: 10.0 ± 0.6; $p > 0.05$, *t*-test).

8. MEMRI scans

In week 10 post CCI-ION model induction when pain behaviors were chronic, anesthetized rats received MEMRI scans conducted 24 hrs after intraperitoneal administration of $MnCl_2$. Images were taken at approximate bregmas 1.00, −1.30, −3.60, and −6.80 mm for comparison between CCI-ION and naïve control animals (Fig. 4A & B, 5A & B). The investigated regions of interest are schematically depicted in the top row of Fig. 4A and 5A.

The MEMRI T1 signal intensity (Fig. 4C), an indicator of neural activity, was significantly different in several ROIs along the pain neuraxis and emotional brain circuitry. Significantly increased T1 signal intensity in the CCI-ION group compared to naïve controls was found for ACC (bilateral), amygdala (ipsilateral / left), dentate gyrus (bilateral), and habenula (bilateral). Significantly decreased T1 signal intensity was recorded for the primary somatosensory cortex barrel field (contralateral / right) and dorsal raphe nucleus (naïve control $n = 3$, CCI-ION $n = 4$, $p < 0.05$, *t*-test). No differences were noted in the thalamic medial dorsal nucleus (MD), reticular nucleus (TRN), and central posteromedial nucleus (VPM) (Supplemental Table 1). Differences between CCI-ION and naïve control group MEMRI T2 signal intensity, which when increased is an indicator of edema or astrogliosis, were also determined for the same ROIs (Fig. 5C). In the CCI-ION group, T2 signal intensity was significantly increased in the ACC (bilateral), habenula (bilateral), and thalamus (bilateral) consisting of VPM and ventral posterolateral nucleus. However, no differences were noted in the thalamic MD, TRN, and VPM (Supplemental Table 2). Significantly reduced T2 signal intensity was recorded in the ventrolateral periaqueductal gray (ipsilateral / left), primary somatosensory cortex barrel field (S1BF) (contralateral / right), and dorsal raphe nucleus when compared to naïve controls indicating increased activation (naïve control $n = 3$, CCI-ION $n = 4$, $p < 0.05$, *t*-test) (Supplemental Table 2).

Based on the behavioral outcomes indicating anxiety-like behavior accompanies chronic pain related behavior in our CCI-ION rat neuropathic pain model, the pain-related aversion

brain circuitry was of particular interest. MEMRI T1 signals in the ipsilateral (left) caudate nucleus of CCI-ION animals were significantly increased compared to naïve controls (CCI-ION ipsilateral = 129.0 ± 0.6, contralateral = 115.6 ± 0.4; naïve ipsilateral = 116.1 ± 1.5, contralateral = 115.4 ± 1.5). Likewise, T2 signals were significantly increased (CCI-ION ipsilateral = 26.8 ± 0.4, contralateral = 22.3 ± 1.1; naïve ipsilateral = 20.5 ± 0.4, contralateral = 20.3 ± 0.6; naïve control $n = 3$, CCI-ION $n = 4$, $p < 0.05$, t-test) (Fig. 6A-C). Measurements from the contralateral (right) caudate nucleus were not different among groups. Bilaterally, the dorsomedial PAG (DMPAG) had significantly higher MEMRI T1 signals in the CCI-ION group compared to the naïve group (CCI-ION ipsilateral = 159.4 ± 0.4, contralateral = 153.5 ± 0.8; naïve ipsilateral = 145.9 ± 1.9, contralateral = 145.8 ± 1.6). The T2 signals were similar (CCI-ION ipsilateral = 28.3 ± 0.4, contralateral = 22.9 ± 0.3; naïve ipsilateral = 18.8 ± 0.3, contralateral = 19.5 ± 0.3) (naïve control $n = 3$, CCI-ION $n = 4$, $p < 0.05$, t-test) (Fig. 6D-F).

9. Discussion

The aim of this study was to demonstrate MEMRI changes in the brain's pain neuraxis and emotional brain circuitry in a chronic pain model 10 weeks post induction. The changes were evident with the concurrent anxiety-like behavior induced at chronic time points in the rat trigeminal neuropathic pain CCI-ION model. As in our previous reports, mechanical hypersensitivity of the whisker pad is maximal 3 weeks post-surgery and remains maximal through the experiment end after week 10 (Ma et al., 2012; Kaushal et al., 2016). The persisting decrease in the head withdrawal threshold is attributable in other models in the literature to central sensitization secondary to primary afferent sensitization. The striking findings of the present study were the anxiety-like behavioral changes and concurrent long-term brain activity changes evident with MEMRI signal intensity. This MEMRI study has identified brain structures active in the long-term "central sensitization" induced by chronic neuropathic pain. The resulting long-term hypersensitivity and anxiety mimics the clinical presentation of chronic pain. The MEMRI signal intensity changes parallel clinical imaging in patients with chronic pain. The results of the study indicate the suitability of this model for further studies of chronic pain and preclinical therapeutic drug testing.

9.1. Chronic pain induced anxiety behaviors

Anxiety-like behaviors reported here at 8 weeks post CCI-ION model induction are equivalent to 4 years of chronic pain in clinical patients (Quinn, 2005; Sengupta, 2013; Dutta and Sengupta, 2016). Long-term hypersensitivity and anxiety-like behavior induced with the CCI-ION model is in contrast to most sciatic nerve tie models. In the light-dark place preference test, CCI-ION animals spent significantly more time in the dark chamber and displayed less exploratory behavior in the light. Similarly, they preferentially stayed in the closed arm and avoided exploring the center of the elevated plus maze assay, measures of anxiety-like behaviors (van Gaalen and Steckler, 2000; File et al., 2004). The incidence of mood disorders such as anxiety and depression is prevalent in patients with chronic pain. Patients with chronic pain are 2.5 to 10 times more likely to suffer also from general anxiety (von Korff et al., 1988; Means-Christensen et al., 2008).

An important feature unique to trigeminal circuitry includes close proximity to brain structures (Xu et al., 2008; Rodriguez et al., 2017). Information from the face pain travels via trigeminal primary afferents through the trigeminal ganglia to synapse in the brainstem medullary dorsal horn as well as to directly innervate the parabrachial complex (Rodriguez et al., 2017). Thus, the trigeminal innervation of the lateral parabrachial nucleus has more direct connectivity, via one synapse, with the limbic system. Spinal input crosses 2 synaptic connections. Optogenetic activation of the trigeminal monosynaptic connectivity was shown to induce escape and avoidance behavior (Rodriguez et al., 2017). Human subjects report increased fear after noxious facial stimulation as compared to similar noxious stimulation of the hand (Schmidt et al., 2016). Secondary axons ascend via the trigeminothalamic and parabrachio-amygdaloid tracts to thalamus and amygdala respectively, then relay to several cortical and subcortical regions including primary and secondary somatosensory cortices, basal ganglia, ACC, and limbic circuitry. Nociceptive information relayed via the basal ganglia is transmitted to the prefrontal cortex and back to the amygdala (Borsook et al., 2010; Tracey and Dickenson, 2012; Bushnell et al., 2013).

9.2. MEMRI activation in supraspinal circuitry

In the present study, we replicated previously used methodology that produced the highest MRI contrast 24 hrs after a single injection of 0.8 mmol/kg $MnCl_2$ (Aoki et al., 2004). Other studies have allowed animals to freely behave for as long as 1-week post $MnCl_2$ injection to better enhance spontaneous pain induced changes in the brain, however, group differences weren't always visible with this method (Devonshire et al., 2017). A downside to the MEMRI method is that Mn^{2+} is a metabolic toxin and competitive Ca^{2+} inhibitor and can be cytotoxic (Lin and Koretsky, 1997; Takeda, 2003). In *in vivo* electrophysiological experiments systemic administration of 0.5 mmol/kg $MnCl_2$ was able to decrease neuronal excitability in the hippocampus (Eschenko et al., 2010). We noticed reduced physiological functions, decreased body temperature and repressed respiration, in some of the studied animals which is why MEMRI scans were performed only once at experiment's end. Quantified MEMRI T1 and T2 signal intensity measurements from chronic CCI-ION and naïve control animals in brain regions involved in the pain circuitry, ascending and descending pain modulation, as well as in regions associated with affective behaviors are compared. A coil artifact was noted in all T1 and T2 scans irrespective of experimental group. To eliminate its influence on the data, we normalized MEMRI T1 and T2 signal intensity measurements to those measured in whole brain for each section prior to taking the mean (Fig. 4 & 5) (Chao et al., 2018).

9.3. Pain circuitry

In the present study, despite continuing hypersensitivity, the MEMRI T1 signal intensity, a measure of neuronal activity (Malheiros et al., 2014), was not significantly different in the thalamus and decreased in S1BF of CCI-ION animals. This is consistent with decreased fMRI BOLD signal in thalamus and cortex of clinical patients with longstanding trigeminal neuropathic pain reportedly associated with gray matter volume decrease in these regions (Gustin et al., 2012; Henderson et al., 2013; Obermann et al., 2013). Youssef et al. (2014) reported decreased regional cerebral blood flow in patients with chronic posttraumatic neuropathy compared to healthy subjects using the more accurate arterial spin labeling MRI

technique, suggesting that dysfunctional central changes and loss of descending inhibition may be essential for maintenance of chronic pain (Henderson et al., 2013). This is in contrast to a study using an acute CCI-ION mouse model that found increased neuronal activity at rest in S1BF using the immunohistochemical neuronal activity biomarkers cFOS and pERK (Thibault et al., 2016). This is suggestive of differential brain activation patterns in acute versus chronic pain.

At the same time, we observed a significant increase of the MEMRI T2 signal intensity, an indicator of tissue water content and possible cellular damage and dysfunction, in the thalamus of CCI-ION animals compared to naïve controls. It is possible that this was due to changes in aquaporin ion channel expression and local edema as was detected after pilocarpine-induced epilepsy in rodents (Malheiros et al., 2014). In contrast, decreased T2 signal intensity in S1BF of CCI-ION animals was similar to reduced T2 relaxometry measured in clinical patients with chronic orofacial pain along the ascending pain pathway (Alshelh et al., 2018). Changes in MEMRI T2 signal intensity are complex and are influenced by Mn^{2+} uptake, changes in water distribution in the tissue. Decreased T2 signal intensity can reflect increased glial activation/astrogliosis as seen after stroke (Justicia et al., 2008). Further histological analyses would be needed to determine anatomical changes contributing to T2 signal intensity changes in CCI-ION animals compared to naïve controls.

Many of the supraspinal brain structures activated in our model at 10 weeks and evident with MEMRI are also reported to be activated by pathological pain in patients. Most of the regions significantly activated in the CCI-ION rats compared to controls are components of the anxiety and aversion circuitry. This is not surprising as even acute noxious stimuli activate not only primary and secondary somatosensory cortices but also elicit neuronal activity in prefrontal and limbic brain regions including ACC, amygdala, and VTA, responsible for affective and contextual associations of pain and pain-related aversion (Tracey and Dickenson, 2012; Ossipov et al., 2014; Boadas-Vaello et al., 2017; Zhao et al., 2018; Meda et al., 2019).

9.4. Amygdala

Significantly increased MEMRI T1 signal intensity was observed in the amygdala of CCI-ION animals compared to controls. This brain region has often been described as contributing to the maintenance of chronic neuropathic pain and anxiety. During acute pain, activation of the amygdala causes the release of the stress-induced hormone corticotropin releasing factor (CRF) and acts as an analgesic. However, during chronic pain when continuous overactivation of the amygdala has caused persistent CRF release, this descending pain modulation no longer functions and its effect may possibly be reversed (Ossipov et al., 2014; Andreoli et al., 2017). Administration of antioxidants or TRPA1 antagonists in the central amygdala nucleus has been shown to inhibit CCI-SN induced hypersensitivity while glial inhibitors had no effect (Sagalajev et al., 2018). Activation of enkephalinergic projection neurons within the central amygdala that synapse in the VLPAG has been shown to not only provide analgesia but to also have anxiolytic effects in mice with somatic neuropathic pain (Paretkar and Dimitrov, 2019).

9.5. ACC

In healthy subjects the ACC is activated by acute pain stimuli (Casey, 1999) and subjects are able to control experimental pain sensation by reducing the neuronal activity within the ACC. This has been demonstrated using fMRI (Bushnell et al., 2013). While healthy subjects do not seek out pain, chronic pain causes pain-related aversion not only in clinical patients but also in animal models during which the ACC plays a critical role. In persistent pain animal models and in clinical patients with pathological pain, neuronal hyperactivity has been measured in the ACC using electrophysiology and imaging studies (Mills et al., 2018; Zhao et al., 2018).

As part of the emotional brain, the ACC encodes the aversive, unpleasant aspects of painful stimuli. Patients with ACC lesions have decreased affective responses to pain (Rainville et al., 1997). The ACC not only contributes to pain sensation and descending pain modulation, but together with the habenula it is involved in negative outcome learning, and as such, contributes to chronic pain associated anxiety (Kawai et al., 2015; Zhao et al., 2018; Meda et al., 2019). The observed increased neuronal activity in the ACC in anesthetized CCI-ION animals demonstrated here with MEMRI is consistent with contribution of the ACC to the maintenance of chronic pain and resulting anxiety-like behaviors.

9.6. Habenula and dorsal raphe nucleus

The habenula, a brain region with axonal connections to the ACC, also had significantly increased T1 signal intensity in CCI-ION animals. This bilateral brain structure is part of the central aversion network involved in a wide range of behaviors including behavioral responses to aversive stimuli such as pain and anxiety (Hikosaka, 2010). The habenula receives direct and indirect afferent pain input from the spinal cord, nucleus accumbens (NAc), frontal cortex, and hypothalamus (Dafny et al., 1996; Craig, 2003; Hikosaka, 2010). Projections from the medial habenula to the interpeduncular nucleus in the midbrain have been shown to be essential for aversive memory formation/retention and fear conditioning (Soria-Gomez et al., 2015; Hsu et al., 2016). Overactivation of the habenular-interpeduncular connectivity during chronic pain could contribute to the development of the anxiety-like behavior in our CCI-ION pain model. The lateral habenula connections to the ACC, medial habenula, and anterior insula form an aversive processing circuit that is central for avoidance learning (Shelton et al., 2012; Vadovicova and Gasparotti, 2013). Increased neuronal excitability in the lateral habenula due to ablation of the KCNQ3 m-type potassium channel subunit increased hyperalgesia caused by alcohol withdrawal in a rat model. Conversely, KCNQ3 overexpression in the lateral habenula decreased hyperalgesia (Kang et al., 2019). In human subjects, chronic stimulation of the lateral habenula disinhibits the ACC, anterior insula, and the pain pathway output, as well as increases learned anxiety and depression (Wang and Aghajanian, 1977; Shabel et al., 2012). The lateral habenula also directly and indirectly regulates monoaminergic neurons within the dorsal raphe nucleus (DRN) where we saw both decreased T1 and T2 relaxation times in CCI-ION animals compared to naïve controls, which suggests regional activation. This lateral habenula-DRN connection, as well as the habenular connection to the locus coeruleus is involved in chronic pain maintenance and anxiety (Herkenham and Nauta, 1979). In healthy animals the activation of dorsomedial neurons within the DRN was reported to be anxiogenic, was

interpreted as suggesting direct involvement of the DRN in regulating anxiety disorders (Spiacci et al., 2016). Further investigation is necessary to confirm that the habenula-DRN connection is a potential limbic drive involved in pain facilitation. The role of serotonin can be both anti- and pro-nociceptive, depending on the receptor subunits it binds to, making the observed decreased T1 and T2 signals from the DRN difficult to interpret. It is possible that the serotonin receptors on which these neurons synapse have changed, interrupting descending pain inhibition and switching to facilitation (D'Mello and Dickenson, 2008; Ossipov et al., 2014). We have previously reported dysfunctional switch from noradrenergic alpha 2 receptor (NAα2R) mediated inhibition to facilitation mediated by NAα1R. We and others have proposed this switch as a responsible factor in chronic hypersensitivity in long-term models after intracerebroventricular or intrathecal injection of specific blockers (Rahman et al., 2008; Kaushal et al., 2016).

9.7. Caudate nucleus and dorsomedial PAG

Other activated supraspinal areas contribute to pain-related aversion behavior. These include the caudate nucleus and DMPAG, regions in which we saw elevated MEMRI T1 signal indicating activation as well as increased T2 signal indicating edema or cell dysfunction. The caudate nucleus is connected to ACC and thalamus and is involved in many different processes ranging from learning and memory formation to pain control (Barker, 1988; Chudler and Dong, 1995). An fMRI study in patients with fibromyalgia demonstrated that cognitive behavioral therapy changes brain activity in response to experimental pain, including an increase in the ipsilateral caudate nucleus (Diers et al., 2012). It is possible that neuronal activation in the caudate of CCI-ION animals reflects descending pain inhibition that in chronic pain states is either ineffective at pain control or has reversed its function to facilitate pain sensation.

The DMPAG also contributes to the emotional aspect of pain, escape behaviors, and descending pain inhibition (Bandler and Shipley 1994; Silva and McNaughton, 2019). Among other brain regions, the DMPAG is closely connected by afferent input from the central amygdala, mPFC, raphe magnus, and A5 noradrenergic cells. In the present study, the T1 MEMRI signal in the VLPAG of CCI-ION animals was not different from controls. In patients with chronic back pain an fMRI study reported that this connectivity is reduced in pain-related fear (Meier et al., 2017). Reduced resting state PAG connectivity with amygdala and insula cortex was also measured in patients with chronic lower back pain and correlated with the severity of the pain, indicating that these connections are essential for descending pain modulation (Yu et al., 2014).

All of the findings presented here support the hypothesis that continued activation of pro-nociceptive pathways results in neural plasticity and activation of supraspinal anxiety and aversion brain circuitry responsible for enhancement and perpetuation of the pain and anxiety related behaviors in our chronic model (Pertovaara et al., 1996; Ossipov et al., 2014).

10. Conclusion

The present study identified both anxiety- and pain-related behaviors in the rat trigeminal chronic constriction injury model of neuropathic pain through week 10 post model induction. At the same 10 week post induction time point, MEMRI identified decreased activity in brain regions involved in descending pain modulation, while neuronal activity increased in aversion and anxiogenic brain regions. These findings parallel the evidence provided by clinical MRI reports that central sensitization during pathological pain involves supraspinal structures of the anxiety and aversion circuitry, while the pain circuitry itself is providing reliable transmission of nociceptive information contralaterally. Thus, study of animal models long-term provides adequate interpretable data for comparison to human studies and is well suited for performing preclinical therapeutic trials.

Supplementary Material

Refer to Web version on PubMed Central for supplementary material.

Acknowledgments

Funding and disclosures

This work was supported by the United States Department of Veterans Administration Merit grant BX002695 (KNW). No authors have conflicts of interest. This communication does not necessarily reflect the views of the Department of Veterans Affairs or the U.S. government.

Abbreviations:

ACC	anterior cingulate cortex
AMYG	amygdala
BOLD	blood oxygen-level dependent
CCI	chronic constriction injury
CRF	corticotropin releasing factor
DEN	dentate gyrus
DMPAG	dorsomedial periaqueductal gray
DRN	dorsal raphe nucleus
FLASH	fast low angle sequence
fMRI	functional magnetic resonance imaging
FOV	field of view
HAB	habenula
ION	infraorbital nerve

MD	medial dorsal nucleus
MEMRI	manganese-enhanced magnetic resonance imaging
mPFC	medial prefrontal cortex
NAα2R	noradrenergic alpha 2 receptor
NAc	nucleus accumbens
PYRC	pyriform cortex
RARE	rapid acquisition with relaxation enhancement
RF	radiofrequency
ROI	region of interest
S1BF	primary sensory cortex barrel field
SN	sciatic nerve
TE	echo time
THAL	thalamus
TR	repetition time
TRN	thalamic reticular nucleus
VLPAG	ventrolateral periaqueductal gray
VPM	ventral posteromedial nucleus
VTA	ventral tegmental area

References

Aloisi AM, Albonetti ME, Carli G, 1994. Sex differences in the behavioural response to persistent pain in rats. Neurosci. Lett 179, 79–82. doi:10.1016/0304-3940(94)90939-3. [PubMed: 7845629]

Alshelh Z, Di Pietro F, Mills EP, Vickers ER, Peck CC, Murray GM, Henderson LA, 2018. Altered regional brain T2 relaxation times in individuals with chronic orofacial neuropathic pain. Neuroimage Clin 19, 167–173. doi:10.1016/j.nicl.2018.04.015. [PubMed: 30035014]

Andreoli M, Marketkar T, Dimitrov E, 2017. Contribution of amygdala CRF neurons to chronic pain. Exp. Neurol 298 (Pt A), 1–12. doi:10.1016/j.expneurol.2017.08.010. [PubMed: 28830762]

Aoki I, Wu YJ, Silva AC, Lynch RM, Koretsky AP, 2004. In vivo detection of neuroarchitecture in the rodent brain using manganese-enhanced MRI. Neuroimage 22, 1046–1059. doi:10.1016/j.neuroimage.2004.03.031. [PubMed: 15219577]

Baliki MN, Petre B, Torbey S, Herrmann KM, Huang L, Schnitzer TJ, Fields HL, Apkarian AV, 2012. Corticostriatal functional connectivity predicts transition to chronic back pain. Nat. Neurosci 15 (8), 1117–1119. doi:10.1038/nn.3153. [PubMed: 22751038]

Bandler R, Shipley MT, 1994. Columnar organization in the midbrain periaqueductal gray: modules for emotional expression? TINS 17 (9), 379–389. [PubMed: 7817403]

Barker RA, 1988. The basal ganglia and pain. Int J Neurosci 41, 29–34. doi:10.3109/00207458808985739. [PubMed: 3045040]

Bedenk BT, Almeida-Corrêa S, Jurik A, Dedic N, Grünecker B, Genewsky AJ, Kaltwasser SF, Riebe CJ, Deussing JM, Czisch M, Wotjak CT, 2018. Mn2+ dynamics in manganese-enhanced MRI (MEMRI): cav1.2 channel-mediated uptake and preferential accumulation in projection terminals. Neuroimage 169, 374–382. doi:10.1016/j.neuroimage.2017.12.054. [PubMed: 29277401]

Boadas-Vaello P, Homs J, Reina F, Carrera A, Verdú E, 2017. Neuroplasticity of Supraspinal Structures Associated with Pathological Pain. Anat Rec (Hoboken) 300 (8), 1481–1501. doi:10.1002/ar.23587. [PubMed: 28263454]

Borsook D, Linnman C, Faria V, Strassman AM, Becerra L, Elman I, 2016. Reward deficiency and anti-reward in pain chronification. Neurosci. Biobehav. Rev 68, 282–297. doi:10.1016/j.neubiorev.2016.05.033. [PubMed: 27246519]

Borsook D, Upadhyay J, Chudler EH, Becerra L, 2010. A key role of the basal ganglia in pain and analgesia - insights gained through human functional imaging. Mol. Pain 6, 27. doi:10.1186/1744-8069-6-27. [PubMed: 20465845]

Bushnell MC, Ceko M, Low LA, 2013. Cognitive and emotional control of pain and its disruption in chronic pain. Nat. Rev. Neurosci 14 (7), 502–511. doi:10.1038/nrn3516. [PubMed: 23719569]

Casey KL, 1999. Forebrain mechanisms of nociception and pain: analysis through imaging. Proc. Natl. Acad. Sci. U. S. A 96 (14), 7668–7674. doi:10.1073/pnas.96.14.7668. [PubMed: 10393878]

Cha M, Lee K, Lee C, Cho JH, Cheong C, Sohn JH, Lee BH, 2016. Manganese-enhanced MR imaging of brain activation evoked by noxious peripheral electrical stimulation. Neurosci. Lett 613, 13–18. doi:10.1016/j.neulet.2015.11.027. [PubMed: 26733299]

Chao TH, Chen JH, Yen CT, 2018. Plasticity changes in forebrain activity and functional connectivity during neuropathic pain development in rats with sciatic spared nerve injury. Mol. Brain 11, 55. doi:10.1186/s13041-018-0398-z. [PubMed: 30285801]

Chaplan SR, Bach FW, Pogrel JW, Chung JM, Yaksh TL, 1994. Quantitative assessment of tactile allodynia in the rat paw. J. Neurosci. Methods 53 (1), 55–63. [PubMed: 7990513]

Chudler EH, Dong WK, 1995. The role of the basal ganglia in nociception and pain. Pain 60, 3–38. doi:10.1016/0304-3959(94)00172-B. [PubMed: 7715939]

Craig AD, 2003. A new view of pain as a homeostatic emotion. Trends Neurosci 26 (6), 303–207. [PubMed: 12798599]

Dafny N, Dong WQ, Prieto-Gomez C, Reyes-Vazquez C, Stanford J, Qiao JT, 1996. Lateral hypothalamus: site involved in pain modulation. Neuroscience 70 (2), 449–460. doi:10.1016/0306-4522(95)00358-4. [PubMed: 8848153]

Danaher RJ, Zhang L, Donley CJ, Laungani NA, Hui SE, Miller CS, Westlund KN, 2018. Histone deacetylase inhibitors prevent persistent hypersensitivity in an orofacial neuropathic pain model. Mol. Pain 14, 1744806918796763. doi:10.1177/1744806918796763.

Devonshire IM, Burston JJ, Xu L, Lillywhite A, Prior MJ, Watson DJG, 2017. Manganese-enhanced magnetic resonance imaging depicts brain activity in models of acute and chronic pain: a new window to study experimental spontaneous pain? Neuroimage 157, 500–510. doi:10.1016/j.neuroimage.2017.06.034. [PubMed: 28633971]

Diers M, Yilmaz P, Rance M, Thieme K, Gracely RH, Rolko C, Schley MT, Kiessling U, Wang H, Flor H, 2012. Treatment-related changes in brain activation in patients with fibromyalgia syndrome. Exp. Brain Res 218 (4), 619–628. doi:10.1007/s00221-012-3055-2. [PubMed: 22427134]

D'Mello R, Dickenson AH, 2008. Spinal cord mechanisms of pain. Br. J. Anaesth 101 (1), 8–16. doi:10.1093/bja/aen088. [PubMed: 18417503]

Dutta S, Sengupta P, 2016. Men and mice: relating their ages. Life Sci 152, 244–248. doi:10.1016/j.lfs.2015.10.025. [PubMed: 26596563]

Eschenko O, Canals S, Simanova I, Logothetis NK, 2010. Behavioral, electrophysiological and histopathological consequences of systemic manganese administration in MEMRI. Magn. Reson. Imaging 28 (8), 1165–1174. doi:10.1016/j.mri.2009.12.022. [PubMed: 20096525]

File SE, Lippa AS, Beer B, Lippa MT, 2004. Animal tests of anxiety. Curr. Protoc. Neurosci doi:10.1002/0471142301.ns0803s26, Chapter 8, Unit 8.3.

Gustin SM, Peck CC, Cheney LB, Macey PM, Murray GM, Henderson LA, 2012. Pain and plasticity: is chronic pain always associated with somatosensory cortex activity and reorganization? J. Neurosci 32 (43), 14874–14884. doi:10.1523/JNEU-ROSCI.1733-12.2012. [PubMed: 23100410]

Hashmi JA, Baliki MN, Huang L, Baria AT, Torbey S, Hermann KM, Schnitzer TJ, Apkarian AV, 2013. Shape shifting pain: chronification of back pain shifts brain representation from nociceptive to emotional circuits. Brain 136 (Pt 9), 2751–2768. doi:10.1093/brain/awt211. [PubMed: 23983029]

Henderson LA, Peck CC, Petersen ET, Rae CD, Youssef AM, Reeves JM, Wilcox SL, Akhter R, Murray GM, Gustin SM, 2013. Chronic pain: lost inhibition? J, Neurosci 33 (17), 7574–7582. doi:10.1523/JNEUROSCI.0174-13.2013. [PubMed: 23616562]

Herkenham M, Nauta WJ, 1979. Efferent connections of the habenular nuclei in the rat. J. Comp. Neurol 187 (1), 19–47. doi:10.1002/cne.901870103. [PubMed: 226566]

Hikosaka O, 2010. The habenula: from stress evasion to value-based decision-making. Nat. Rev. Neurosci 11 (7), 503–513. doi:10.1038/nrn2866. [PubMed: 20559337]

Hsu YW, Morton G, Guy EG, Wang SD, Turner EE, 2016. Dorsal Medial Habenula Regulation of Mood-Related Behaviors and Primary Reinforcement by TachykininExpressing Habenula Neurons. eNeuro. 3 (3). doi:10.1523/ENEURO.0109-16.2016, pii: ENEURO.0109-16.2016.

Justicia C, Ramos-Cabrer P, Hoehn M, 2008. MRI detection of secondary damage after stroke: chronic iron accumulation in the thalamus of the rat brain. Stroke 39 (5), 1541–1547. doi:10.1161/STROKEAHA.107.503565. [PubMed: 18323485]

Kang S, Li J, Zuo W, Chen P, Gregor D, Fu R, Han X, Bekker A, Ye JH, 2019. Downregulation of M-channels in lateral habenula mediates hyperalgesia during alcohol withdrawal in rats. Sci. Rep 9 (1), 2714. doi:10.1038/s41598-018-38393-7. [PubMed: 30804373]

Kaushal R, Taylor BK, Jamal AB, Zhang L, Ma F, Donahue R, Westlund KN, 2016. GABA-A receptor activity in the noradrenergic locus coeruleus drives trigeminal neuropathic pain in the rat; contribution of NAα1 receptors in the medial prefrontal cortex. Neuroscience 334, 148–159. doi:10.1016/j.neuroscience.2016.08.005. [PubMed: 27520081]

Kawai T, Yamada H, Sato N, Takada M, Matsumoto M, 2015. Roles of the Lateral Habenula and Anterior Cingulate Cortex in Negative Outcome Monitoring and Behavioral Adjustment in Nonhuman Primates. Neuron 88 (4), 792–804. doi:10.1016/j.neuron.2015.09.030. [PubMed: 26481035]

Kline RH 4th, Exposto FG, O'Buckley SC, Westlund KN, Nackley AG, 2015. Catechol-O-methyltransferase inhibition alters pain and anxiety-related volitional behaviors through activation of β-adrenergic receptors in the rat. Neuroscience 290, 561–569. doi:10.1016/j.neuroscience.2015.01.064. [PubMed: 25659347]

LaPaglia DM, Sapio MR, Burbelo PD, Thierry-Mieg J, Thierry-Mieg D, Raithel SJ, Ramsden CE, Iadarola MJ, Mannes AJ, 2018. RNA-Seq investigations of human post-mortem trigeminal ganglia. Cephalalgia 38 (5), 912–932. doi:10.1177/0333102417720216. [PubMed: 28699403]

Lin YJ, Koretsky AP, 1997. Manganese ion enhances T1-weighted MRI during brain activation: an approach to direct imaging of brain function. Magn. Reson. Med 38 (3), 378–388. [PubMed: 9339438]

Lu C, Yang T, Zhao H, Zhang M, Meng F, Fu H, Xie Y, Xu H, 2016. Insular Cortex is Critical for the Perception, Modulation, and Chronification of Pain. Neurosci. Bull 32 (2), 191–201. doi:10.1007/s12264-016-0016-y. [PubMed: 26898298]

Ma F, Zhang L, Lyons D, Westlund KN, 2012. Orofacial neuropathic pain mouse model induced by Trigeminal Inflammatory Compression (TIC) of the infraorbital nerve. Mol. Brain 5, 44. doi:10.1186/1756-6606-5-44. [PubMed: 23270529]

Malheiros JM, Persike DS, Castro LU, Sanches TR, Andrade Lda C, Tannús A, Covolan L, 2014. Reduced hippocampal manganese-enhanced MRI (MEMRI) signal during pilocarpine-induced status epilepticus: edema or apoptosis? Epilepsy Res 108 (4), 644–652. doi:10.1016/j.eplepsyres.2014.02.007. [PubMed: 24630048]

Mansour AR, Baliki MN, Huang L, Torbey S, Herrmann KM, Schnitzer TJ, Apkarian AV, 2013. Brain white matter structural properties predict transition to chronic pain. Pain 154 (10), 2160–2168. doi:10.1016/j.pain.2013.06.044. [PubMed: 24040975]

Massaad CA, Pautler RG, 2011. Manganese-enhanced magnetic resonance imaging (MEMRI). Methods Mol. Biol 711, 145–174. doi:10.1007/978-1-61737-992-5_7. [PubMed: 21279601]

Maves TJ, Pechman PS, Gebhart GF, Meller ST, 1993. Possible chemical contribution from chromic gut sutures produces disorders of pain sensation like those seen in man. Pain 54 (1), 57–69 Erratum in: Pain 1993, 55 (1), 131–134. [PubMed: 8378104]

May A, 2008. Chronic pain may change the structure of the brain. Pain 137 (1), 7–15. doi:10.1016/j.pain.2008.02.034. [PubMed: 18410991]

McCarberg B, Peppin J, 2019. Pain Pathways and Nervous System Plasticity: learning and Memory in Pain. Pain Med. doi:10.1093/pm/pnz017, pii: pnz017.

Means-Christensen AJ, Roy-Byrne PP, Sherbourne CD, Craske MG, Stein MB, 2008. Relationships among pain, anxiety, and depression in primary care. Depress. Anxiety. 25 (7), 593–600. doi:10.1002/da.20342. [PubMed: 17932958]

Meda KS, Patel T, Braz JM, Malik R, Turner ML, Seifikar H, Basbaum AI, Sohal VS, 2019. Microcircuit Mechanisms through which Mediodorsal Thalamic Input to Anterior Cingulate Cortex Exacerbates Pain-Related Aversion. Neuron 102 (5), 944–959. doi:10.1016/j.neuron.2019.03.042, e3. [PubMed: 31030955]

Meier ML, Stämpfli P, Humphreys BK, Vrana A, Seifritz E, Schweinhardt P, 2017. The impact of pain-related fear on neural pathways of pain modulation in chronic low back pain. Pain Rep 2 (3), e601. doi:10.1097/PR9.0000000000000601. [PubMed: 29392216]

Mills EP, Di Pietro F, Alshelh Z, Peck CC, Murray GM, Vickers ER, Henderson LA, 2018. Brainstem Pain-Control Circuitry Connectivity in Chronic Neuropathic Pain. J. Neurosci 38 (2), 465–473. doi:10.1523/JNEUROSCI.1647-17.2017. [PubMed: 29175957]

Mutso AA, Petre B, Huang L, Baliki MN, Torbey S, Herrmann KM, Schnitzer TJ, Apkarian AV, 2014. Reorganization of hippocampal functional connectivity with transition to chronic back pain. J. Neurophysiol 111 (5), 1065–1076. doi:10.1152/jn.00611.2013. [PubMed: 24335219]

Nahin RL, 2017. Severe Pain in Veterans: the Effect of Age and Sex, and Comparisons With the General Population. J. Pain 18 (3), 247–254. doi:10.1016/j.jpain.2016.10.021. [PubMed: 27884688]

Obermann M, Rodriguez-Raecke R, Naegel S, Holle D, Mueller D, Yoon MS, Theysohn N, Blex S, Diener HC, Katsarava Z, 2013. Gray matter volume reduction reflects chronic pain in trigeminal neuralgia. Neuroimage 74, 352–358. doi:10.1016/j.neuroimage.2013.02.029. [PubMed: 23485849]

Ong WY, Stohler CS, Herr DR, 2019. Role of the Prefrontal Cortex in Pain Processing. Mol. Neurobiol 56 (2), 1137–1166. doi:10.1007/s12035-018-1130-9. [PubMed: 29876878]

Ossipov MH, Morimura K, Porreca F, 2014. Descending pain modulation and chronification of pain. Curr. Opin. Support. Palliat. Care 8 (2), 143–151. doi:10.1097/SPC.0000000000000055. [PubMed: 24752199]

Paretkar T, Dimitrov E, 2019. Activation of enkephalinergic (Enk) interneurons in the central amygdala (CeA) buffers the behavioral effects of persistent pain. Neurobiol. Dis 124, 364–372. doi:10.1016/j.nbd.2018.12.005. [PubMed: 30572023]

Pautler RG, 2004. In vivo, trans-synaptic tract-tracing utilizing manganese-enhanced magnetic resonance imaging (MEMRI). NMR Biomed 17 (8), 595–601. [PubMed: 15761948]

Paxinos G, Watson C, 1996. The Rat Brain in Stereotaxic Coordinates. Academic Press, San Diego 3rd ednPp. xxxiii+80; ISBN 0 12 547623.

Pertovaara A, Wei H, Hämäläinen MM, 1996. Lidocaine in the rostroventromedial medulla and the periaqueductal gray attenuates allodynia in neuropathic rats. Neurosci. Lett 218 (2), 127–130. doi:10.1016/s0304-3940(96)13136-0. [PubMed: 8945744]

Quinn R, 2005. Comparing rat's to human's age: how old is my rat in people years? Nutrition. United States 21 (6), 775–777. doi:10.1016/j.nut.2005.04.002.

Rahman W, D'Mello R, Dickenson AH, 2008. Peripheral nerve injury-induced changes in spinal alpha(2)-adrenoceptor-mediated modulation of mechanically evoked dorsal horn neuronal responses. J. Pain 9 (4), 350–359. doi:10.1016/j.jpain.2007.11.010. [PubMed: 18226963]

Rainville P, Duncan GH, Price DD, Carrier B, Bushnell MC, 1997. Pain affect encoded in human anterior cingulate but not somatosensory cortex. Science 277 (5328), 968–971. doi:10.1126/science.277.5328.968. [PubMed: 9252330]

Rodriguez E, Sakurai K, Xu J, Chen Y, Toda K, Zhao S, Han BX, Ryu D, Yin H, Liedtke W, Wang F, 2017. A craniofacial-specific monosynaptic circuit enables heightened affective pain. Nat.

Neurosci 20 (12), 1734–1743. doi:10.1038/s41593-017-0012-1, Erratum in: Nat. Neurosci. 2018 Mar 16. [PubMed: 29184209]

Sagalajev B, Wei H, Chen Z, Albayrak I, Koivisto A, Pertovaara A, 2018. Oxidative Stress in the Amygdala Contributes to Neuropathic Pain. Neuroscience 387, 92–103. doi:10.1016/j.neuroscience.2017.12.009. [PubMed: 29274353]

Saville D, 1990. Multiple Comparison Procedures: the Practical Solution. Am Stat 44 (2), 174–180. doi:10.2307/2684163.

Schmidt K, Forkmann K, Sinke C, Gratz M, Bitz A, Bingel U, 2016. The differential effect of trigeminal vs. peripheral pain stimulation on visual processing and memory encoding is influenced by pain-related fear. Neuroimage 134, 386–395. doi:10.1016/j.neuroimage.2016.03.026. [PubMed: 27015710]

Seminowicz DA, Laferriere AL, Millecamps M, Yu JS, Coderre TJ, Bushnell MC, 2009. MRI structural brain changes associated with sensory and emotional function in a rat model of long-term neuropathic pain. Neuroimage 47 (3), 1007–1014. doi:10.1016/j.neuroimage.2009.05.068. [PubMed: 19497372]

Sengupta P, 2013. The Laboratory Rat: relating Its Age With Human's. Int. J. Prev. Med 4 (6), 624–630. [PubMed: 23930179]

Shabel SJ, Proulx CD, Trias A, Murphy RT, Malinow R, 2012. Input to the lateral habenula from the basal ganglia is excitatory, aversive, and suppressed by serotonin. Neuron 74, 475–481. doi:10.1016/j.neuron.2012.02.037. [PubMed: 22578499]

Shelton L, Becerra L, Borsook D, 2012. Unmasking the mysteries of the habenula in pain and analgesia. Prog. Neurobiol 96 (2), 208–219. doi:10.1016/j.pneurobio.2012.01.004. [PubMed: 22270045]

Silva C, McNaughton N, 2019. Are periaqueductal gray and dorsal raphe the foundation of appetitive and aversive control? A comprehensive review. Prog. Neurobiol 177, 33–72. doi:10.1016/j.pneurobio.2019.02.001. [PubMed: 30786258]

Soria G, Wiedermann D, Justicia C, Ramos-Cabrer P, Hoehn M, 2008. Reproducible imaging of rat corticothalamic pathway by longitudinal manganese-enhanced MRI (L-MEMRI). Neuroimage 41 (3), 668–674. doi:10.1016/j.neuroimage.2008.03.018. [PubMed: 18445533]

Soria-Gómez E, Busquets-Garcia A, Hu F, Mehidi A, Cannich A, Roux L, Louit I, Alonso L, Wiesner T, Georges F, Verrier D, Vincent P, Ferreira G, Luo M, Marsicano G, 2015. Habenular CB1 Receptors Control the Expression of Aversive Memories. Neuron 88 (2), 306–313. doi:10.1016/j.neuron.2015.08.035. [PubMed: 26412490]

Spiacci A Jr., Pobbe RLH, Matthiesen M, Zangrossi H Jr., 2016. 5-HT1A receptors of the rat dorsal raphe lateral wings and dorsomedial subnuclei differentially control anxiety- and panic-related defensive responses. Neuropharmacology 107, 471–479. doi:10.1016/j.neuropharm.2015.06.015. [PubMed: 26145183]

Takeda A, 2003. Manganese action in brain function. Brain Res. Brain Res. Rev 41 (1), 79–87. [PubMed: 12505649]

Thibault K, Rivière S, Lenkei Z, Férézou I, Pezet S, 2016. Orofacial Neuropathic Pain Leads to a Hyporesponsive Barrel Cortex with Enhanced Structural Synaptic Plasticity. PLoS ONE 11 (8), e0160786. doi:10.1371/journal.pone.0160786. [PubMed: 27548330]

Tracey I, Dickenson A, 2012. SnapShot: pain perception. Cell 148 (6), 1308. doi:10.1016/j.cell.2012.03.004, e2. [PubMed: 22424237]

Vadovičová K, Gasparotti R, 2013. Reward and adversity processing circuits, their competition and interactions with dopamine and serotonin signaling. ScienceOpen Res doi:10.14293/S2199-1006.1.SORLIFE.AEKZPZ.v1, arXiv:1304.4201.

van Gaalen MM, Steckler T, 2000. Behavioural analysis of four mouse strains in an anxiety test battery. Behav. Brain Res 115 (1), 95–106. [PubMed: 10996412]

Von Korff M, Dworkin SF, Le Resche L, Kruger A, 1988. An epidemiologic comparison of pain complaints. Pain 32 (2), 173–183. [PubMed: 3362555]

Vos BP, Strassman AM, Maciewicz RJ, 1994. Behavioral evidence of trigeminal neuropathic pain following chronic constriction injury to the rat's infraorbital nerve. J. Neurosci 14 (5 Pt 1), 2708–2723. [PubMed: 8182437]

Wang RY, Aghajanian GK, 1977. Physiological evidence for habenula as major link between forebrain and midbrain raphe. Science 197, 89–91. doi:10.1126/science.194312. [PubMed: 194312]

Xu M, Aita M, Chavkin C, 2008. Partial infraorbital nerve ligation as a model of trigeminal nerve injury in the mouse: behavioral, neural, and glial reactions. J. Pain 9, 1036–1048. doi:10.1016/j.jpain.2008.06.006. [PubMed: 18708302]

Youssef AM, Gustin SM, Nash PG, Reeves JM, Petersen ET, Peck CC, Murray GM, Henderson LA, 2014. Differential brain activity in subjects with painful trigeminal neuropathy and painful temporomandibular disorder. Pain 155 (3), 467–475. doi:10.1016/j.pain.2013.11.008. [PubMed: 24269492]

Yu R, Gollub RL, Spaeth R, Napadow V, Wasan A, Kong J, 2014. Disrupted functional connectivity of the periaqueductal gray in chronic low back pain. Neuroimage Clin 6, 100–108. doi:10.1016/j.nicl.2014.08.019. [PubMed: 25379421]

Zhao R, Zhou H, Huang L, Xie Z, Wang J, Gan WB, Yang G, 2018. Neuropathic Pain Causes Pyramidal Neuronal Hyperactivity in the Anterior Cingulate Cortex. Front. Cell. Neurosci 12, 107. doi:10.3389/fncel.2018.00107. [PubMed: 29731710]

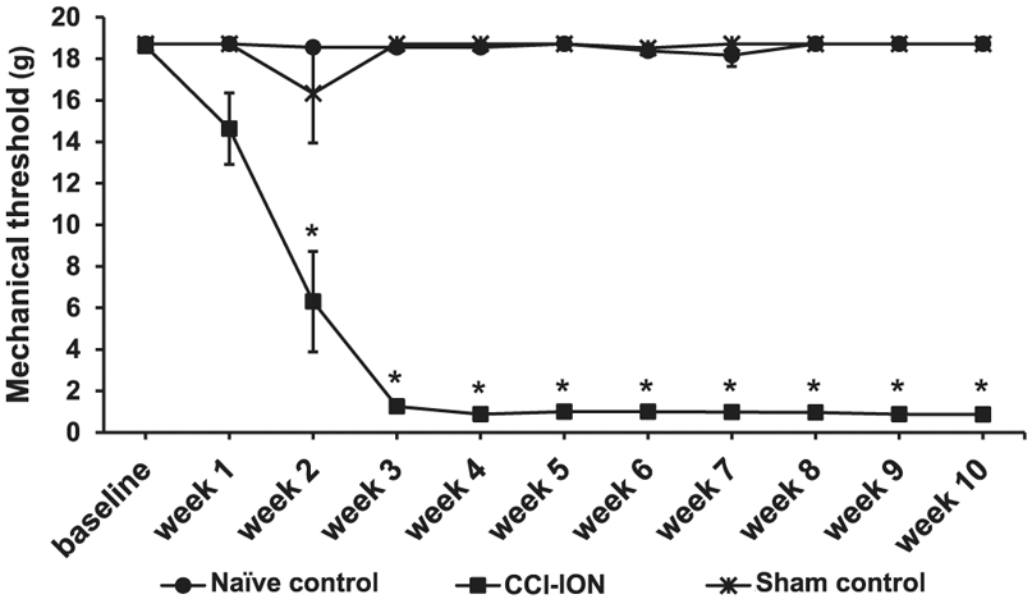

Fig. 1.

Mechanical withdrawal thresholds on the ipsilateral/left whisker pad were significantly reduced within 2 weeks in rats with CCI-ION injury. This hypersensitivity was maximal by week 3 and persisted until experiment's end in week 10. Repeated mechanical testing alone did not change the mechanical withdrawal thresholds of naïve and sham surgery control animals. $n = 6$ per group; * $p < 0.05$, one-way ANOVA. .

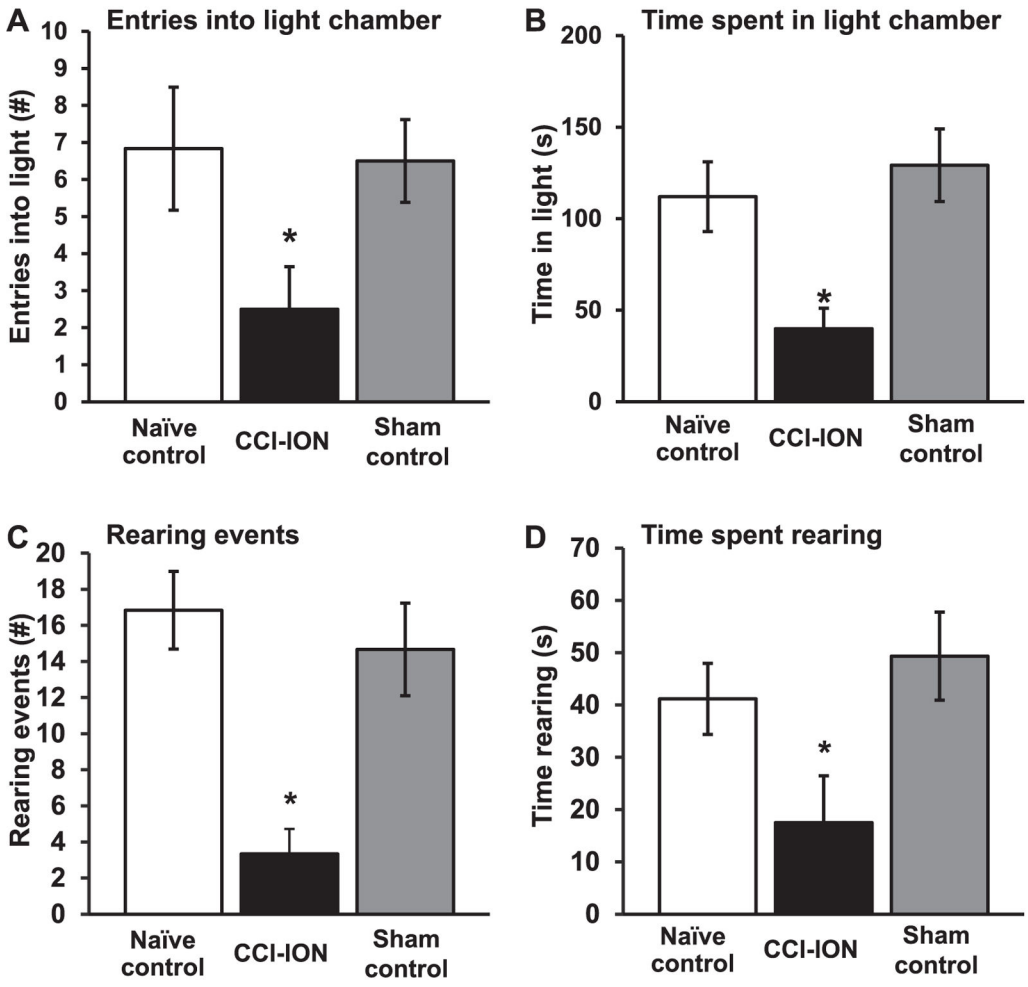

Fig. 2.

Eight weeks after CCI-ION trigeminal nerve injury, animals displayed anxiety-like behavior in the light-dark place preference test. (**A**) CCI-ION animals entered the brightly illuminated chamber significantly less often and (**B**) spent significantly less time there. (**C**) Exploratory rearing events of CCI-ION animals and (**D**) time spent rearing in the light chamber were also significantly less compared to naïve and sham control animals. $n = 6$ per group; * $p < 0.05$, one-way ANOVA.

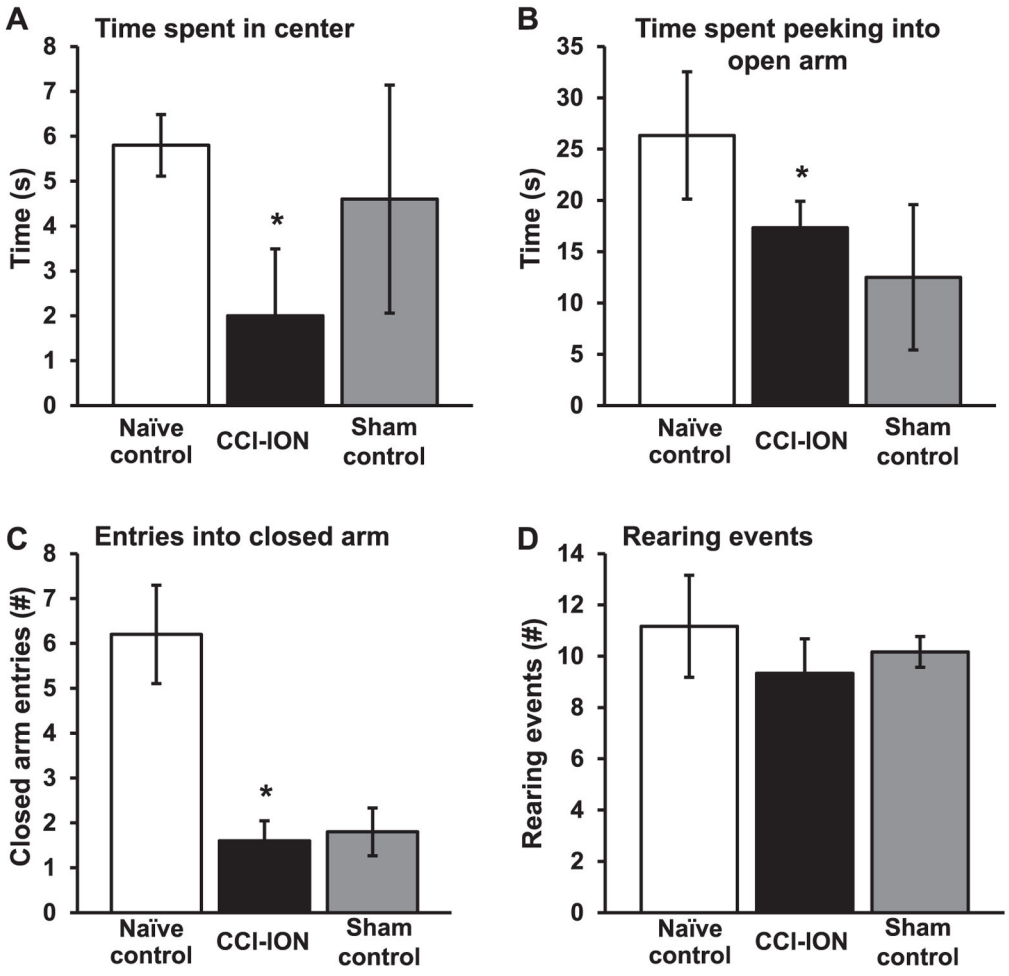

Fig. 3.

In week 9 post trigeminal nerve injury, CCI-ION animals displayed anxiety-like behavior in the elevated plus maze. CCI-ION animals spent significantly less time (**A**) in the center, (**B**) peeking into the open arm, and (**C**) entered the closed arm less often compared to naïve controls, though analysis indicated no difference from sham controls. (**D**) The number of rearing events was not different between groups. $n = 6$ per group; * $p < 0.05$, one-way ANOVA.

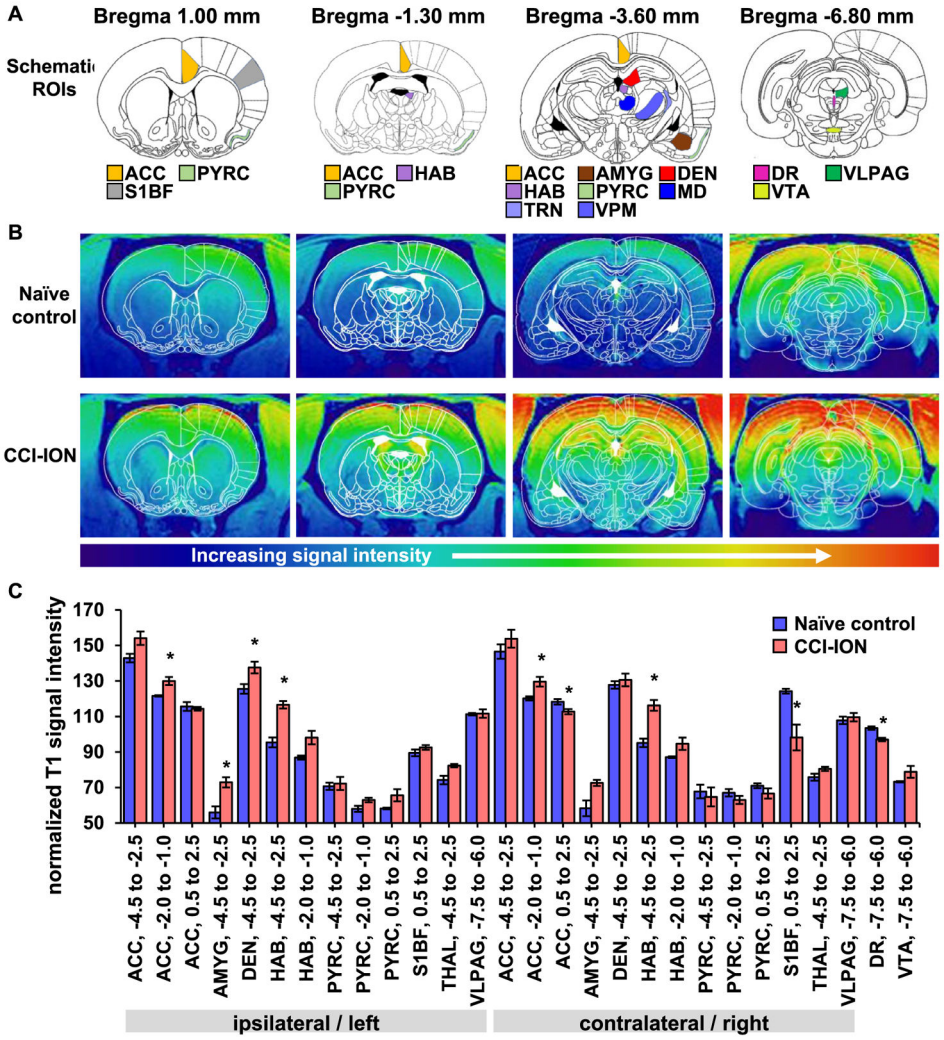

Fig. 4.

The MEMRI T1 signal intensity, indicators of neural activity, in CCI-ION animals were significantly different from naïves with regional specificity, with some brain regions having significant increased and others decreased signals. (**A**) Location of analyzed ROIs drawn into images from the Paxinos & Watson rat brain atlas (1996). (**B**) Representative T1 MEMRI images of a sample naïve control and CCI-ION animal at bregma 1.00, −1.30, −3.60, and −6.80 mm with superimposed cytoarchitecture from the Paxinos & Watson rat brain atlas (1996). Excessive dorsal image brightness is due to a coil artifact. (**C**) The MEMRI T1 signal intensity, normalized to whole brain signal intensity in CCI-ION rats, is plotted for regions of interest (ROIs) within the pain neuraxis and emotional brain circuitry. The normalized T1 signal intensity in CCI-ION rats was significantly greater in ACC (bilateral), amygdala (ipsilateral / left), dentate gyrus (bilateral), and habenula (bilateral) and was significantly reduced in the primary somatosensory cortex barrel field (contralateral / right) and dorsal raphe nucleus. Bregma locations (in mm) are written after each ROI abbreviation. Naïve control $n = 3$, CCI-ION $n = 4$, * $p < 0.05$, *t*-test. ACC, anterior cingulate cortex; AMYG, amygdala; DEN, dentate gyrus; DRN, dorsal raphe nucleus;

HAB, habenula; PYRC, pyriform cortex; S1BF, primary sensory cortex barrel field; THAL, thalamus; VLPAG, ventrolateral periaqueductal gray; VTA, ventral tegmental area.

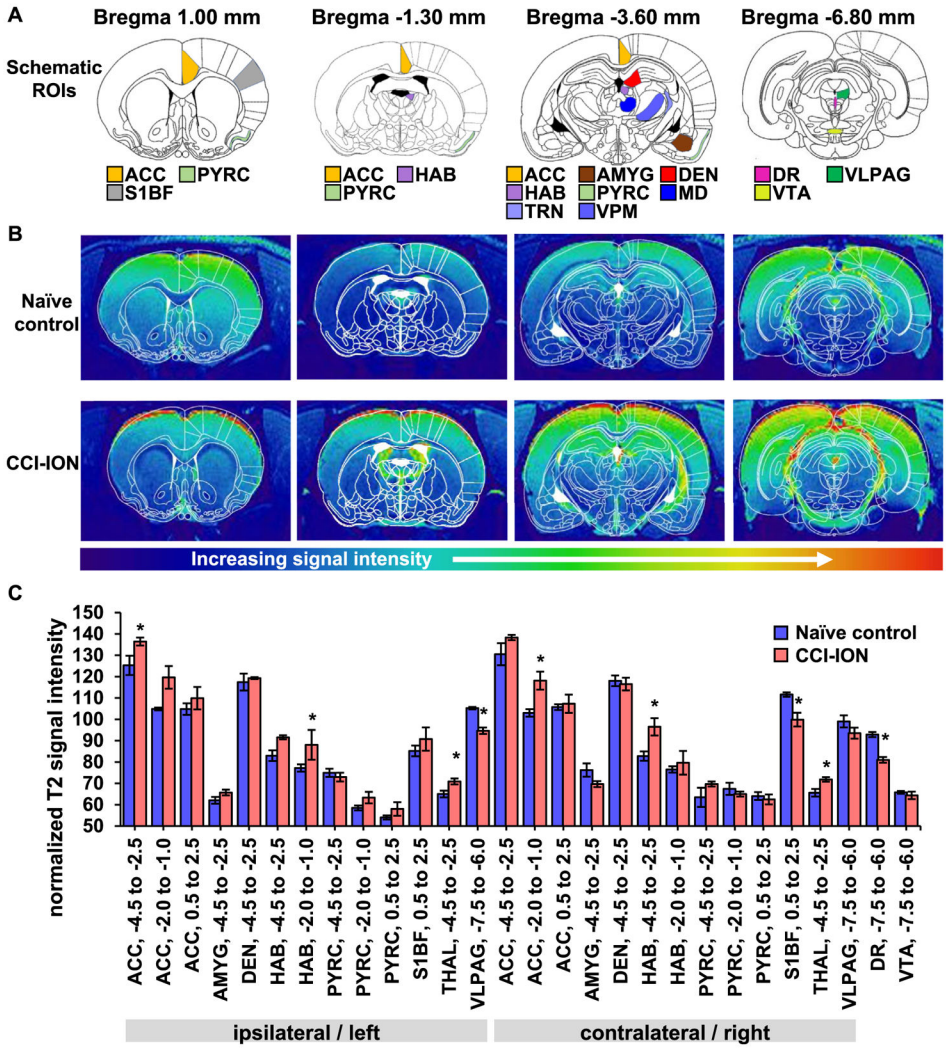

Fig. 5.

The MEMRI T2 signal intensity measured in CCI-ION animals differed significantly from naïve controls in several ROIs along the pain neuraxis and emotional brain circuitry. (**A**) Location of analyzed ROIs drawn into images from the Paxinos & Watson rat brain atlas (1996). (**B**) Representative T2 MEMRI images of a sample naïve control and CCI-ION animal are shown at bregma 1.00, −1.30, −3.60, and −6.80 mm with superimposed images from the Paxinos & Watson rat brain atlas (1996). Excessive dorsal image brightness is due to a coil artifact. (**C**) The T2 signal intensity was normalized to whole brain in CCI-ION rats and plotted for ROIs within the pain neuraxis and emotional brain circuitry. The normalized T2 signal intensity in CCI-ION rats was significantly greater in ACC (bilateral), habenula (bilateral) and thalamus (bilateral), but was significantly reduced in primary ventrolateral periaqueductal gray (ipsilateral / left), somatosensory cortex barrel field (contralateral / right) and dorsal raphe nucleus. Bregma location (in mm) are written behind ROI abbreviation. Naïve control $n = 3$, CCI-ION $n = 4$, * $p < 0.05$, *t*-test. ACC, anterior cingulate cortex; AMYG, amygdala; DEN, dentate gyrus; DRN, dorsal raphe

nucleus; HAB, habenula; PYRC, pyriform cortex; S1BF, primary sensory cortex barrel field; THAL, thalamus; VLPAG, ventrolateral periaqueductal gray; VTA, ventral tegmental area.

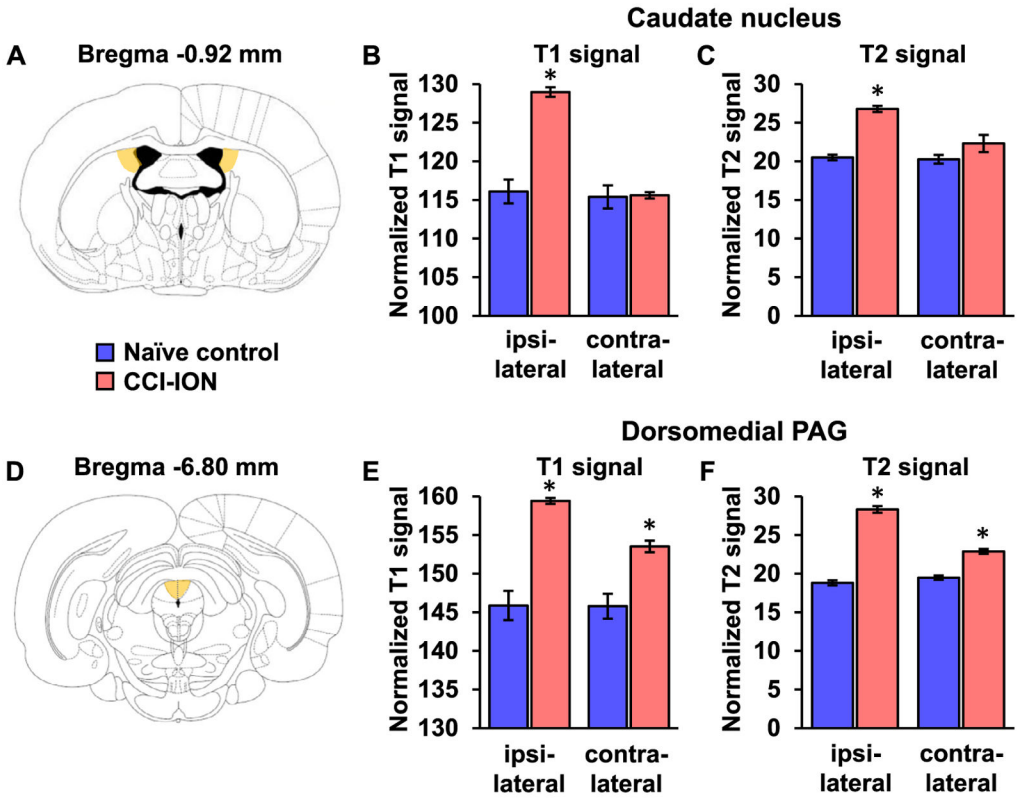

Fig. 6.

In animals with chronic CCI-ION injury, MEMRI T1 and T2 signals were increased in pain-related aversion brain centers, the caudate nucleus and DMPAG. (**A**) Schematic of the caudate nucleus ROIs are at bregma −0.92 mm (from Paxinos and Watson, 1996). In CCI-ION animals (**B**) the T1 signal and (**C**) T2 signal are significantly increased in the ipsilateral / left caudate nucleus compared to naïve controls, but not different on the contralateral / right side. (**D**) Schematic of ROIs of the DMPAG ROIs located at bregma −6.80 mm (from Paxinos and Watson, 1996). (**E**) The MEMRI T1 and (**F**) T2 signals were bilaterally increased in the CCI-ION animals compared to naïve controls. Naïve control $n = 3$, CCI-ION $n = 4$, * $p < 0.05$, t-test.